

## Transverse Resistance in Two-Dimensional Electron Gas in Oblique Lateral Superlattice

Mayumi KATO, Akira ENDO, Shingo KATSUMOTO\*  
and Yasuhiro IYE\*

*Institute for Solid State Physics, University of Tokyo, Roppongi,  
Minato-ku, Tokyo 106-8666*

(Received May 24, 1999)

KEYWORDS: 2DEG, lateral superlattice, transverse resistivity,  
umklapp process, GaAs/AlGaAs

Two-dimensional electron gas (2DEG) at GaAs/AlGaAs heterointerface is one of the systems best suited for studies of basic transport processes. The band structure in the relevant energy range is isotropic and parabolic so that a free-electron-like model is well justified. Samples with electron mean free path in excess of tens of micrometers are available, so that with modern microfabrication techniques it is not difficult to fabricate various artificial structures with the length scale much smaller than the mean free path. Electron transport in such artificial structures has been extensively investigated to uncover a wide variety of phenomena.<sup>1)</sup>

Recently, we and other workers have shown that a 2DEG subjected to a lateral magnetostatic superlattice, i.e. a spatially periodic magnetic field modulation with zero uniform component, exhibits an excess resistivity, which shows a characteristic  $T^2$ -dependence at low temperatures.<sup>2-4)</sup> The  $T^2$ -term is attributed to the electron-electron umklapp scattering, which is absent in a plain 2DEG but can occur in the presence of the imposed periodic potential. In this paper, we show that the same process gives rise to a transverse resistivity component, when the artificial superlattice is made oblique. i.e. when the direction of modulation is set at an angle with respect to the transport current. We also show that the similar phenomenon occurs for the case of lateral electrostatic superlattice.

The samples were fabricated from a GaAs/AlGaAs single heterojunction wafer with carrier density  $n_e \approx 3.4 \times 10^{15} \text{ m}^{-2}$  and mobility  $\mu \approx 60 \text{ m}^2/\text{Vs}$  at 4.2 K. The depth of the heterointerface from the top surface was 75 nm. The sample geometry is schematically shown in the upper left inset of Fig. 1. A standard Hall bar pattern was defined by photolithography and wet chemical etching, and the ohmic contacts were made by AuGe alloying. A grating gate electrode was fabricated on top of the current channel of the Hall bar, by electron beam lithography, thermal evaporation of thin film metal and lift-off process. The grating gate consisted of cobalt metal strips with thickness 60 nm and width 250 nm, placed at a 500 nm period. These parameters were the same as

those for one of the samples used in our previous study.<sup>3)</sup> The difference is in the orientation of the grating pattern. The Hall bar was oriented with the current channel parallel to the [110] direction, and the grating pattern was oriented along the [100] direction so that the modulation wave vector is at  $45^\circ$  with respect to the current direction. The reason for setting the grating pattern parallel to the [100] direction was to minimize the built-in potential modulation due to strain via the piezoelectric coupling.<sup>5,6)</sup> The transport measurements were carried out by a standard low frequency a.c. technique with a constant current bias. Both the longitudinal and transverse voltages were measured. A cross coil superconducting magnet system and a rotating sample holder were used to apply an external magnetic field at any angle with precision better than  $0.01^\circ$ .

We measured the longitudinal and transverse resistivity components with an external field  $H = 5 \text{ T}$  applied exactly parallel to the 2DEG plane and parallel to the modulation wave vector (i.e. perpendicular to the long side of the strips). The cobalt wires are fully magnetized by the external field and their fringing field creates a sinusoidally varying perpendicular magnetic field component at the 2DEG plane. The amplitude of the magnetic field modulation for this configuration is estimated as  $B_0 \approx 52 \text{ mT}$  from our previous study. The effect of the lateral magnetic superlattice in this case manifests itself as an increase in the longitudinal resistivity and as a non-zero transverse resistivity component, even though the uniform component of the magnetic field is zero. The lower right inset of Fig. 1 shows the temperature dependence of the longitudinal resistivity in the presence and absence of the magnetic field modulation. The excess longitudinal resistivity  $\Delta\rho_{xx}$  is defined as the difference between the two data, and is plotted against  $T^2$  in the main panel with solid circles. They obey the relation  $\Delta\rho_{xx}(T) = AT^2 + C$ , as we reported in our previous papers.<sup>2,3)</sup> Also shown here is the transverse resistivity  $\rho_{xy}$  (open circles), which occurs only in the case of oblique lateral superlattice. It is seen that the relation  $|\rho_{xy}(T)| = \Delta\rho_{xx}(T)$  holds very well in the present case of  $45^\circ$  oblique grating. This is a clear piece of evidence that both the transverse resistivity and the excess longitudinal resistivity are caused by the same back scattering process. Namely, the umklapp backscattering vector makes an angle  $45^\circ$  with the current vector, so that each back scattering event contributes equally to the longitudinal and transverse components of the electric field. Numerically,  $|\rho_{xy}(T)| = \Delta\rho_{xx}(T) = 11.0 + 0.040(T[\text{K}])^2 [\Omega]$  for  $B_0 = 52 \text{ mT}$ .

Next we turn to the case of electrostatic modulation.<sup>7)</sup> For this measurement, we demagnetized the ferromagnetic gate and changed the gate bias at zero magnetic field. The inset of Fig. 2 shows the gate bias dependence of  $\rho_{xx}$  and  $\rho_{xy}$  at 1.2 K. With increasing negative gate bias,  $\rho_{xx}$  increases and  $\rho_{xy}$  becomes non-zero, even though no magnetic field is involved at all. The situation here is somewhat more complicated than the case of magnetic modulation, because the gate bias changes not only the electrostatic modulation amplitude but also the electron density, so that the quantity  $\Delta\rho_{xx}$  cannot

\* Also at CREST, Japan Science and Technology Corporation, Mejiro, Toshima-ku, Tokyo 171-0031.

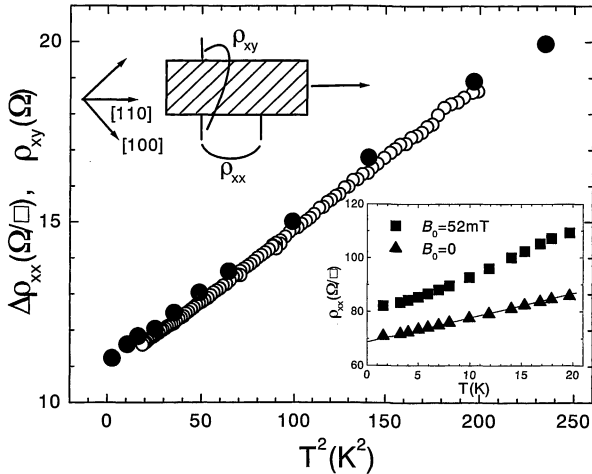


Fig. 1. The upper left inset schematically shows the sample configuration. The lower right inset shows the temperature dependences of the resistivities in the presence and absence of the spatially alternating magnetic field. The difference of the two sets of data gives the excess resistivity  $\Delta\rho_{xx}$  due to the lateral magnetic superlattice. The main panel shows the excess longitudinal resistivity  $\Delta\rho_{xx}$  (solid circles) and the transverse resistivity  $\rho_{xy}$  (open circles) as a function of  $T^2$ .

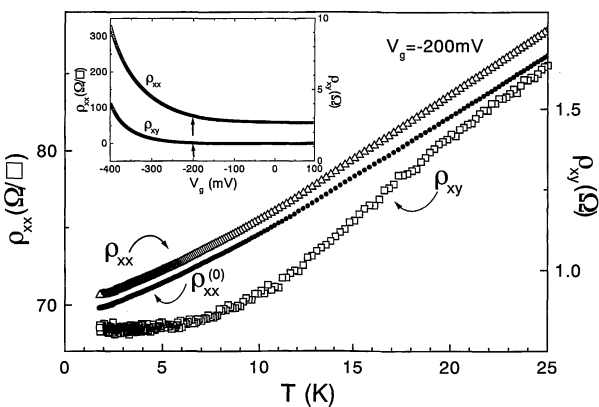


Fig. 2. The inset shows the longitudinal resistivity  $\rho_{xx}$  and the transverse resistivity  $\rho_{xy}$  as a function of the gate bias  $V_g$ . The main panel shows the temperature dependences of  $\rho_{xx}$  (triangles, left scale) and  $\rho_{xy}$  (squares, right scale) with the gate bias fixed at  $V_g = -200$  mV (marked by arrows in the inset). The small dots represent  $\rho_{xx}^{(0)} = \rho_{xx} - |\rho_{xy}|$  which corresponds to the resistivity after subtracting the effect of the lateral superlattice.

be extracted so straightforwardly as the case of magnetic superlattice.

The main panel of Fig. 2 shows  $\rho_{xx}(T)$  and  $\rho_{xy}(T)$  for the gate bias  $V_g = -200$  mV. The electron density at this gate bias determined from the Hall data is  $n_e = 3.2 \times 10^{15} \text{ m}^{-2}$ , which is a little lower than  $n_e = 3.4 \times 10^{15} \text{ m}^{-2}$  at  $V_g = 0$ . As seen in the inset, the resistivity change in this range of the gate bias is small, so that the effect of the lateral electric superlattice can be treated as perturbation. It is seen that  $\rho_{xy}(T)$  shows a  $T^2$  dependence, while  $\rho_{xx}(T)$  shows behavior close to  $T$ -linear. Numerically,  $\rho_{xy} = 0.82 + 0.0016 (T[\text{K}])^2 [\Omega]$  for  $V_g = -200$  mV. Based on the result for the lateral magnetic superlattice, we assume that  $|\rho_{xy}(T)| = \Delta\rho_{xx}(T)$ , and evaluate the quantity  $\rho_{xx} - |\rho_{xy}|$ , which corresponds to  $\rho_{xx}^{(0)} = \rho_{xx} - \Delta\rho_{xx}$ , i.e. the resistivity excluding the effect of the lateral superlattice, which is shown by small dots in Fig. 2. The  $\rho_{xx}^{(0)}$  thus obtained is not so differ-

ent from  $\rho_{xx}$  for the present case of weak modulation. The temperature dependence of  $\rho_{xx}^{(0)}$  is approximately  $T$ -linear, which can be naturally attributed to acoustic phonon scattering. Indeed, the coefficient of the  $T$ -linear term of the inverse mobility  $1/\mu$  is calculated as  $\alpha = 3.3 \times 10^{-8} \text{ V}_S/\text{cm}^2 \text{ K}$  and is in good agreement with those reported in the literature.<sup>8)</sup> We note however that unlike the case of magnetic modulation,  $\rho_{xx}^{(0)}(T)$  of the 2DEG under electrostatic modulation shows some deviation from the  $T$ -linear behavior of a plain 2DEG.

The deviation from the simple picture becomes more evident, as the gate bias is set more negative. Firstly, the temperature dependence of  $\rho_{xx}^{(0)} = \rho_{xx} - |\rho_{xy}|$  deviates further from the  $T$ -linear behavior and becomes increasingly superlinear. Secondly,  $\rho_{xy}$  at low temperature deviates from the  $T^2$ -dependence. Under a large negative bias,  $\rho_{xy}$  even shows an upturn at the lowest temperatures. These anomalous features are presumably associated with the following. A large negative bias both decreases the Fermi energy and increases the electrostatic modulation amplitude. When the latter becomes a significant fraction of the former, the perturbative treatment breaks down. It is necessary to take account of the spatial inhomogeneity of the electron density. Another factor is that the effect of disorder gains importance with decreasing electron density. In order to interpret the experimental data in the large negative bias region, these factors have to be properly taken into account.

To summarize, we have shown that the oblique lateral superlattice can induce the transverse component of resistivity in 2DEG. In the case of magnetostatic superlattice, where the modulation can be turned on and off without affecting the electron density, the relation  $|\rho_{xy}(T)| = \Delta\rho_{xx}(T)$  expected for in the  $45^\circ$  oblique lateral superlattice is experimentally confirmed, testifying that the excess resistivity is indeed caused by the umklapp process in the periodic structure. Similar effect is observed in the electric superlattice, but the behavior at larger modulation amplitude has some unexplained features that call for further study.

We thank Prof. H. Fukuyama for helpful conversations.

- 1) See for example, C. W. J. Beenakker and H. van Houten: *Solid State Phys.*, **44**, ed. H. Ehrenreich and D. Turnbull (Academic Press, San Diego, 1991) p. 1; S. Datta: *Electronic Transport in Mesoscopic Systems* (Cambridge University Press, Cambridge, 1995).
- 2) M. Kato, A. Endo and Y. Iye: *Phys. Rev. B* **58** (1998) 4876.
- 3) M. Kato, A. Endo and Y. Iye: *J. Phys. Soc. Jpn.* **68** (1999) 1492.
- 4) N. Overend, A. Nogaret, B. L. Gallagher, P. C. Main, R. Wirtz, R. Newbury, M. A. Howson and S. P. Beaumont: *Physica B* **249–251** (1998) 326.
- 5) E. Skuras, A. R. Long, I. A. Larkin, J. H. Davies and M. C. Holland: *Appl. Phys. Lett.* **70** (1997) 871.
- 6) A. Nogaret, S. Carlton, B. L. Gallagher, P. C. Main, M. Henini, R. Wirtz, R. Newbury, M. A. Howson and S. P. Beaumont: *Phys. Rev. B* **55** (1997) 16037.
- 7) A. Messica, A. Soibel, U. Meirav, A. Stern, H. Shtrikman, V. Umansky and D. Mahalu: *Phys. Rev. Lett.* **78** (1997) 705.
- 8) E. E. Mendez, P. J. Price and M. Heiblum: *Appl. Phys. Lett.* **45** (1984) 294; B. J. F. Lin, D. C. Tsui and G. Weimann: *Solid State Commun.* **56** (1985) 287.